Lung Cancer 183 (2023) 107308

Contents lists available at ScienceDirect

Lung Cancer

journal homepage: www.elsevier.com/locate/lungcan

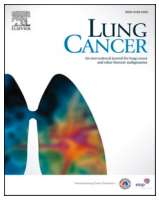

Gene-network analysis predicts clinical response to immunotherapy in patients affected by NSCLC

Federico Cucchiara [a], Stefania Crucitta [a], Iacopo Petrini [b,c], Diego de Miguel Perez [d], Martina Ruglioni [a], Eleonora Pardini [c], Christian Rolfo [d,*], Romano Danesi [a,*], Marzia Del Re [a,d]

[a] Unit of Clinical Pharmacology and Pharmacogenetics, Department of Clinical and Experimental Medicine, University of Pisa, Pisa, Italy
[b] Cardiothoracic and Vascular Department, University of Pisa, Pisa, Italy
[c] Unit of General Pathology, Department of Translational Research and New Technologies in Medicine and Surgery, University of Pisa, Pisa, Italy
[d] Center for Thoracic Oncology, Tisch Cancer Institute, Icahn School of Medicine at Mount Sinai, New York, NY, United States

ARTICLE INFO

Keywords:
Co-occurring mutations
Gene network analysis
Biomarkers
Immunotherapy
NSCLC

ABSTRACT

Objectives: Predictive biomarkers of response to immune checkpoint inhibitors (ICIs) have been extensively studied in non-small cell lung cancer (NSCLC) with controversial results. Recently, gene-network analysis emerged as a new tool to address tumor biology and behavior, representing a potential tool to evaluate response to therapies.

Methods: Clinical data and genetic profiles of 644 advanced NSCLCs were retrieved from cBioPortal and the Cancer Genome Atlas (TCGA); 243 ICI-treated NSCLCs were used to identify an immunotherapy response signatures *via* mutated gene network analysis and K-means unsupervised clustering. Signatures predictive values were tested in an external dataset of 242 cases and assessed versus a control group of 159 NSCLCs treated with standard chemotherapy.

Results: At least two mutations in the coding sequence of genes belonging to the chromatin remodelling pathway (A signature), and/or at least two mutations of genes involved in cell-to-cell signalling pathways (B signature), showed positive prediction in ICI-treated advanced NSCLC. Signatures performed best when combined for patients undergoing first-line immunotherapy, and for those receiving combined ICIs.

Conclusions: Alterations in genes related to chromatin remodelling complexes and cell-to-cell crosstalk may force dysfunctional immune evasion, explaining susceptibility to immunotherapy. Therefore, exploring mutated gene networks could be valuable for determining essential biological interactions, contributing to treatment personalization.

1. Introduction

Non-Small Cell Lung Cancer (NSCLC) treatment for advanced-stage disease recently underwent remarkable changes, first with targeted therapies and, in the last years, with the introduction of immune checkpoint inhibitors (ICIs). In terms of biomarkers, the clinical benefit of first line pembrolizumab is greater for patients with advanced NSCLC when PD-L1 expression is $\geq$ 50% in cancer cells [1]. While, in subsequent-lines, pembrolizumab demonstrated clinical benefit in patients with PD-L1 expression $\geq$ 1% of tumor cells [2]. Moreover, only about 20% of unselected patients respond to these treatments [1–7], highlighting the unreliable nature of PD-L1 expression as predictive biomarker of clinical benefit. Other anti-PD-1/PD-L1 have been approved for the treatment of patients with advanced NSCLC regardless of PD-L1 expression [5,8]. Therefore, additional biomarkers have been investigated, including serum molecules, peripheral blood cells, and tumor-infiltrating lymphocytes (TILs) [9]. The tumor mutational burden (TMB) is the most studied biomarker, which is defined as the total number of somatic/acquired mutations per tumor genome coding area (Mut/Mb). The higher the TMB, the greater the therapeutic effect of PD-1/PD-L1 inhibitors [10]. Despite being scientifically intriguing, TMB lacks compelling clinical data and has shown several limitations to its

* Corresponding authors at: Unit of Clinical Pharmacology and Pharmacogenetics, Department of Clinical and Experimental Medicine, University Hospital of Pisa, Via Roma 55, 56126 Pisa, Italy, (Romano Danesi); Center for Thoracic Oncology, Tisch Cancer Institute, Icahn School of Medicine at Mount Sinai, 1 Gustave L. Levy Pl, NY 10029 New York, United States (Christian Rolfo).
E-mail addresses: christian.rolfo@mssm.edu (C. Rolfo), romano.danesi@unipi.it (R. Danesi).

https://doi.org/10.1016/j.lungcan.2023.107308
Received 13 May 2023; Received in revised form 23 June 2023; Accepted 14 July 2023
Available online 16 July 2023

potential adoption in clinical practice [11]. Historically, TMB has been evaluated by whole-exome sequencing (WES), looking for the entire coding regions [12]. However, it is unrealistic to do WES analysis for all immunotherapy candidate patients due to the high cost of the procedure, despite several comprehensive gene panels have been developed to use next-generation sequencing (NGS). Nonetheless, analyses remain expensive, and despite the efforts to standardize TMB calculation, the reproducibility of results across laboratories is still poor. Moreover, there is no clear consensus on the TMB cutoff for patient stratification [13,14], and intratumor heterogeneity and subsequent spatially divergent mutational profiles influence TMB estimation [15]. Conversely, a TMB-related signature of somatic mutations could be considered a more stable and reliable biomarker: they are few, categorical (binary, the abnormalities are either present or absent), and may be the driver of tumor progression and proliferation. Therefore, a network of functionally significant alterations, dialoguing between each other (gene-network), may be a more powerful biomarker than a summary of all mutant genes harboured by a tumour (TMB). In detail, gene networks may be considered as diagrams consisting of nodes, which represent mutated genes, and edges, which represent pair-wise relationships between mutated genes. When mutated, some hub genes increased their degree in the tumor network compared to their degree in the normal network, suggesting their regulatory role in cancer [16].

The present study proposes to classify NSCLC based on relational patterns (i.e., networks) of mutated genes with great value for prediction of response to immunotherapy. Exploring these networks could be a valuable tool to determine essential biological interactions of mutated genes, contributing to patient classification and personalized treatment decisions.

2. Materials and Methods

2.1. Data collection

cBioPortal for Cancer Genomics web resource (RRID: SCR_014555, http://www.cbioportal.org/) [17,18] was used to explore, visualize, and obtain multidimensional data from NSCLC patients. Data from published studies [19–23] were downloaded to create the group receiving immunotherapy. Patients were then randomly assigned to a training or test set. At the same time, all NSCLCs with genomic and clinical data available on The Cancer Genome Atlas (TCGA, RRID: SCR_003193) [24–26] have been included to create a control group of patients treated with standard chemotherapy. Data were retrieved *via* the Bioconductor (RRID: SCR_006442) R package TCGABiolinks [27]. Clinical information included patient demographics, smoking history, tumor type, disease status, therapeutic management, and survival data. The datasets also retained sampled tumors' details, such as PD-L1 expression and molecular profiles (i.e., mutations count, TMB, insertion/deletions, copy number variations).

Clinical features and genes tested for somatic alterations common between studies were selected. Data from patients with localized disease and treated in the neoadjuvant/adjuvant setting combined with surgery or radiotherapy were removed. Further, patients undergoing target therapy or immunotherapy were excluded from the control group.

The study populations underwent tumor and germline DNA sequencing using either the Memorial Sloan Kettering (MSK)-IMPACT targeted sequencing assay [19,22] or whole-exome sequencing (WES) [20,21,23–26]. However, subsequent analyses considered only the 341 genes included in the MSK-IMPACT panel. Tumor tissues were obtained from the primary or metastatic site, stage III-IV, lung adenocarcinoma (LUAD), and squamous cell carcinoma (LUSC). Samples were either formalin-fixed paraffin-embedded (FFPE) or flash frozen material and were collected for sequencing before dosing with ICIs.

Overlaps were avoided. For duplicate patients appearing in different datasets, duplicate data were crossed out while non-overlapping information were used to replenish the database. Whenever possible, missing data from the cBioPortal downloaded datasets have been completed using supplementary information from published articles.

2.2. General statistics and data preparing

Clinical categorical variables - sex, smoking habits, tumor subtype, tumor stage at diagnosis, PD-L1 score, treatments received, line of therapy, and patient clinical outcome - have been described by absolute and relative frequencies; quantitative factors such as age, smoking pack-years, and TMB by mean ± standard deviation. Data were compared using the χ2-test for categorical variables and Spearman's correlation/Mann-Whitney *U* test for continuous variables. The study's primary endpoint was the PFS, computed from the date of initiation of immunotherapy to the date of progression or death by any cause, as assessed and documented in the selected studies. Also, durable clinical benefit (DCB) was defined as responsive/stable disease lasting $\geq$ 6 months. Secondary endpoints included the overall survival (OS), intended from the first-line treatment start date to death by any cause. Patients were scored censored if they did not reached the outcome of interest. PFS and OS were illustrated using the Kaplan-Meier method and log-rank tests. Cox proportional hazard models evaluated hazard ratio (HR) and 95% confidence interval (CI). The Oncoprint feature of cBioPortal [17,18] was used to visualize individual genetic alterations of each selected patient comprehensively. cBioPortal algorithms like GISTIC or RAE were used to define copy number alterations (CNAs). Deep deletions and amplifications as biologically relevant for individual genes by default were considered. The Bioconductor R package Maftools [28] was used to efficiently describe and analyse somatic variants and CNAs.

2.3. Delineating mutated gene networks and analysis

To calculate the extent to which mutated gene networks might predict the survival of patients undergoing immunotherapy, an R (R Foundation for Statistical Computing, Vienna, Austria) approach was designed to use baseline molecular information in the cases training data set. Custom scripts have been associated with confirmed packages available from CRAN or Bioconductor. The pipeline is available for free upon request to the authors.

The workflow was developed in 2 parts: 1) determining the relationship networks between mutated genes and their analysis; 2) mutated genes unsupervised clustering and survival analyses.

Firstly, results were retrieved from the cBioPortal exclusive/co-occurring event analysis. The study considered all the possible pairings between the MSK-IMPACT panel genes within the training dataset. The Odds Ratio (OR) distribution of the events (co-occurrence/mutual exclusivity) was normalized by taking the respective log2 and considered against the related p-value. Only positive co-occurrence relationships were selected based on the strength of their association. To achieve minimal spurious co-occurrences and avoid subsequent network distortion, pairs of mutated genes were supposed to be meaningful if they showed significant co-occurrence ($p < 0.05$) and the respective Log2OR was greater than +3.

Therefore, an adjacency list was created to identify a network of mutated genes, thanks to the igraph R package [29]. The first two columns of the adjacency list reported paired mutated genes (i.e., the network's nodes). Also, a non-zero numeric value in the third column of the list indicated the presence of an edge between the nodes and corresponded to their respective co-occurrence Log_2OR value.

The network was plotted, and statistics were produced to describe the position and connectedness of mutated genes within the network, including the *Degree, Betweenness, Closeness, Eigen Centrality, and Bonacich Power* [30]. The Degree indicates the number of connections of one with other mutated genes and is a way of measuring gene *activity* within the network. The Betweenness is a more complex trait that counts the number of times a mutated gene is on the shortest path among other mutated genes. The Betweenness characterizes how much control a

mutated gene can exert within the nearby network (its *centrality*).

Mutated genes are nodes within the gene network. The Closeness measures the average proximity of a node to every other network node, which is a way to measure its *efficiency*. The Eigen Centrality also assesses the number of connections of one with other nodes within the network. However, unlike Degree and by calculating the extended links of a node, Eigen Centrality can identify the *influence* of a mutated gene on the whole network, and not just direct connections.

In 1987 Bonacich proposed that even Power was a function of the connections of the mutated genes in one's neighborhood, to be described together with centrality. The more the connections between nodes in the mutated gene nearby network, the more central the mutated gene is. The fewer the links, the more *powerful* it is.

2.4. Unsupervised clustering and survival analyses

After z-standardized the distributions of the above network statistics as they failed the Shapiro-Wilk test, a series of filters were performed to select mutated genes with relevance for survival. Mutated genes with spurious connections to the nearby and whole network were removed while accepted if the following requirements were met: 1) z-Degree > -0.5 (z-Degree ranged from −1.24 to 3.08); 2) z-Betweenness > -0.5 (z-Betweenness ranged from −1 to 6.79 respectively); 3) z-Eigen Centrality > -0.5 (z-Eigen Centrality ranged from −0.77 to 3.42); 4) z-proximity > -0.5 (z-proximity ranged from −2.88 to 2.39). Further, to reduce false-positive calls of non-essential variants to the network, mutated genes were preserved when their z-Bonacich Power ranged from −2.53 to 3.02, excluding those whose value was between −0.5 and 0.5.

Taking advantage of these features, an unsupervised machine learning clustering algorithm (K-means) [31] was used to group 65 mutated genes significantly connected.

Degree, Betweenness, Closeness, Eigen Centrality, and Bonacich Power offered a multidimensional description of genes that needed preprocessing with Principal Component Analysis (PCA) [32,33]. PCA removed noise by reducing the number of predictors to a weighted combination that captures as much information as possible, i.e., the principal components (PCs). PCs are orthogonal projections of data into lower-dimensional space. PC1 is computed to explain the original features' most significant variance (within-cluster sum of squared errors). PC2, orthogonal to PC1, presents the most significant variance left after PC1. PC3, orthogonal to PC1 and PC2, explains the most significant variance left after PC1 and PC2, and so on.

A K-means algorithm was fitted on the top two PCs using Caret, Kernlab, and Factoextra R-packages to obtain an insightful clustering. Of the many K-Means clustering variants, the most popular one – the Lloyd algorithm – was used [34,35]. K-means automatically uncovered the underlying data structure among mutated genes and partitioned them into the desired number (K) of non-overlapping clusters based on their similarity concerning normalized Degree, Betweenness, Closeness, Eigen Centrality, and Bonacich Power. The optimal number of clusters was determined through the Elbow method [36]. The elbow method plots the variance against the number of clusters. First clusters will introduce a lot of variance and information, but the information gain will become low at some point, thus giving the graph an elbow angle. This point (i.e., the *elbow point*) suggests the optimal number of clusters.

Mutated genes were clustered into three distinct groups based on the elbow criterion. Only genes altered in more than five patients were assumed to describe a signature. Patients were deemed signature-positive if they harbored mutations in at least two genes from one of the three groups.

Results from the cases' training set were verified to match an independent validation test set. Therefore, patients receiving immunotherapy were compared with controls undergoing chemotherapy only.

2.5. Enrichment analysis

Finally, ShinyGO v0.76 [37] and the Gene Set Enrichment Analysis (GSEA) [38] were used to get mechanistic facts about the clustered gene lists. ShinyGO found pathways involving signature-related genes by analysing their functional enrichment. Additionally, GSEA conduction determined whether mutated cancer genes were differentially expressed and involved in activating/silencing specific biological pathways more than expected by chance. The Broad Institute's Cancer Cell Line Encyclopedia (CCLE) portal was explored to retrieve mRNA expression profiling (corrected by reads per kilobase per million reads, RPKM) of 16192 between genes and respective variants of 92 NSCLC cell lines - for which the mutational status of signature-related genes had already been investigated. As for patients, cell lines were considered signature-positive if they harbored mutations in at least two genes from one of the three pre-identified gene sets. Statistically significant and concordant differences between signature-positive and signature-negative cell lines were studied using GSEA by focusing on well-defined biological states or processes of the *hallmark molecular signatures* collection [39] from the Molecular Signatures Database (MSigDB). GSEA software can be downloaded from https://www.gsea-msigdb.org/gsea/downloads.jsp after login. Also, molecular signatures to use with GSEA can be recovered from https://www.gsea-msigdb.org/gsea/msigdb/index.jsp.

Statistical analyses were also performed using the free and open statistical software program JAMOVI® (RRID: SCR_016142, https://www.jamovi.org/). Differences were considered significant at $p < 0.05$.

3. Results

3.1. Patients' clinical traits

The study included a total of 485 patients, collected from different studies (Supplementary Fig. 1). Clinical data and somatic mutations were retrieved from the cBioPortal for Cancer Genomics web resource (http://www.cbioportal.org/) [17,18]. Case clinical traits are summarized in Table 1.

The median follow-up was 21.7 months (95% CI 20.0–24.9). Two hundred fifteen patients died, 154 were still alive, and 116 were lost at the follow-up. All patients had advanced stage (III/IV) NSCLC and were treated with anti-PD-1, anti-CTLA-4, or a combination of ICI. Overall, median OS was 12.6 months (95% CI 11–15.5), and median PFS was 4.63 (95% CI 3.80–5.57). Patients who received first-line ICIs had a better median PFS (7.82 months) and OS (46 months) than those who undertook second- (median PFS of 3.43 months, $p < 0.001$; median OS of 16 months, $p = 0.003$), or third-/subsequent-line immunotherapy (median PFS of 2.90 months, $p < 0.001$; median OS of 13 months, $p = 0.001$) (Supplementary Fig. 2A and B). Similarly, when combined, ICIs combined proved to perform better than the monotherapy, and patients reported a median PFS of 7.75 vs 4.17 months ($p < 0.001$). Also, patients undergoing combined ICIs did not reach a median OS value, unlike those treated as monotherapy (median OS 12 months, $p = 0.015$; Supplementary Fig. 3A and B). Queried genes were altered in 475 (98%) of cases. There were 4300 mutations in the coding sequence, excluding silent mutations. Missense mutations were 3265, 435 nonsense, 3 STOP codon, 9 loss-of-codon START, 305 frameshift IN/DELs, and 90 in-frame IN/DELs. One hundred ninety-three mutations were in the splice sites (Fig. 1A); a median of 7 mutations was observed for each patient (range 2–89; Fig. 1B). In addition, 37 genes harboured copy number aberrations: 28 and 6, respectively, showed high-level copy number increase and loss, while three genes showed both (Fig. 1C). *TP53* was mutated in most cases (59%), followed by *KRAS* (33%), *KEAP1* and *STK11* (20%), *EGFR* (15%), *PTPRD* (12%), *SMARCA4* (11%) and *KMT2D* (10%) (Supplementary Fig. 4).

Table 1
Clinical characteristics of patients.

	CASES				CONTROLS	*Cases vs. Controls p-value*
	Training-set	Test-set	*Traning- vs. Test-set p-value*	Overall	Overall	
N° of patients	**243**	**242**		**485**	**159**	
AGE						
Missing	10	6		16	3	
Mean (SD), years	65.1 (10.2)	65.2 (10.7)	*0.992*	65.2 (10.4)	65.1 (9.7)	*0.973*
SEX						
Female	128(52.7%)	127 (52.5%)	*0.966*	255 (52.6%)	67 (42.1%)	*0.022*
Male	115 (47.3%)	115 (47.5%)		230 (47.4%)	92 (57.9%)	
SMOKING HISTORY						
Missing	72	56		128	9	
Ever	139 (81.3%)	143 (76.9%)	*0.307*	282 (79.0%)	135 (90.0%)	*0.003*
Never	32 (18.7%)	43 (23.1%)		75 (21.0%)	15 (10.0%)	
SMOKING PACK-YEARS						
Missing	215	208		423	39	
Mean (SD), pack-years	24.2 (19.8)	25.3 (24.3)	*0.932*	24.8 (22.2)	45.3 (32.0)	*<0.001*
CANCER SUBTYPE						
LUAD	207 (85.2%)	205 (84.7%)	*0.884*	412 (84.9%)	89 (56.0%)	*<0.001*
LUSC	36 (14.8%)	37 (15.3%)		73 (15.1%)	70 (44.0%)	
TUMOR STAGE						
Advanced (Stage III-IV)	243 (100.0%)	242 (100.0%)	*1*	485 (100.0%)	159 (100.0%)	*1*
SAMPLE TYPE						
Missing	71	68		139	2	
Metastasis	94 (54.7%)	89 (51.1%)	*0.514*	183 (52.9%)	0 (0%)	*<0.001*
Primary	78 (45.3%)	85 (48.9%)		163 (47.1%)	157 (100.0%)	
TMB						
Mean (SD), Mut/Mb	10.0 (11.0)	9.3 (9.0)	*0.448*	9.6 (10.1)	9.3 (7.7)	*0.366*
PD-L1 SCORE						
Missing	161	146		307	159	
Negative	29 (35.4%)	42 (43.8%)	*0.333*	71 (39.9%)	–	–
Strong	16 (19.5%)	21 (21.9%)		37 (20.8%)	–	
Weak	37 (45.1%)	33 (34.4%)		70 (39.3%)	–	
INVESTIGATED THERAPY TYPE						
anti-PD-1(Pembrolizumab)	194 (79.8%)	184 (76.0%)	*0.313*	378 (77.9%)	–	*<0.001*
anti-PD-1 plus anti-CTLA-4 (nivolumab plus ipilimumab)	49 (20.2%)	58 (24.0%)		107 (22.1%)	–	
Chemotherapy	–	–		–	159 (100.0%)	
LINE OF THERAPY						
Missing	88	69		157		
1	60 (38.7%)	70 (40.5%)	*0.91*	130 (39.6%)	159 (100.0%)	–
2	59 (38.1%)	66 (38.2%)		125 (38.1%)	0 (0%)	
≥3	36 (23.2%)	37 (21.4%)		73 (22.3%)	0 (0%)	
DURABLE CLINICAL BENEFIT						
Missing	89	78		167	159	
NO	94 (61.0%)	96 (58.5%)	*0.649*	190 (59.7%)	–	–
YES	60 (39.0%)	68 (41.5%)		128 (40.3%)	–	

Categorical variables are described by absolute and relative frequencies, while quantitative factors by mean ± standard deviation (SD). Abbreviation: LUAD, Lung Adenocarcinoma; LUSC, Lung Squamous Cell Carcinoma; TMB, Tumor Mutational Burden; Mut/Mb, mutations per megabase; PD-1, programmed death 1 protein; PD-L1, programmed death ligand 1 protein; CTLA-4, Cytotoxic T-Lymphocyte Associated Protein 4.

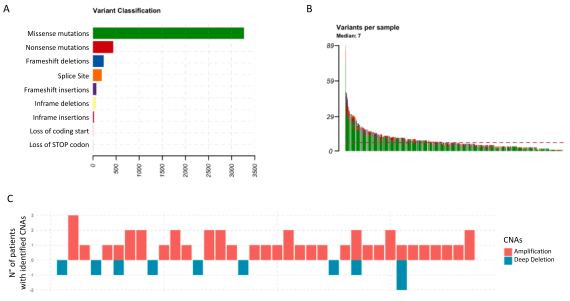

Fig. 1. Characteristics of variants identified in the 485 NSCLC cases underwent immunotherapy. (A) Bar chart showing the absolute counts of variants across NSCLC cases, grouped by type. (B) Histogram showing the cumulative frequency of variants for individual cases (on the x-axis). The median number of mutations per sample is 7. (C) Bar chart showing absolute counts of CNAs among patients.

3.2. Classification of NSCLC patients according to their altered genes

The training data set was used to develop the clustering model of relations between altered genes. To achieve minimal spurious co-occurrences and avoid subsequent network distortion, an exclusive/co-occurring event analysis considered all 57,970 possible pairings between the 341 genes of the MSK-IMPACT panel. As a result, 2683 significant pairs of mutated genes were selected to describe the gene network (Fig. 2A). Unessential genes to the network were filtered-out through distribution normalization of degree, betweenness, closeness, Eigen Centrality, and Bonacich Power analysis. Among the selected 65 genes, network features related directly, to define a complex five-dimensional structure: Degree and Betweenness (Spearman's ρ 0.60, $p < 0.001$), Degree and Closeness (Spearman's ρ 0.94, $p < 0.001$), Degree and Eigen Centrality (Spearman's ρ 0.89, $p < 0.001$), Closeness and Betweenness (Spearman's ρ 0.61, $p < 0.001$), Closeness and Eigen Centrality (Spearman's ρ 0.85, $p < 0.001$), Eigen Centrality and Betweenness (Spearman's ρ 0.41, $p < 0.001$) (Supplementary Fig. 5A-B).

To avoid the "curse of dimensionality" while preserving the overall

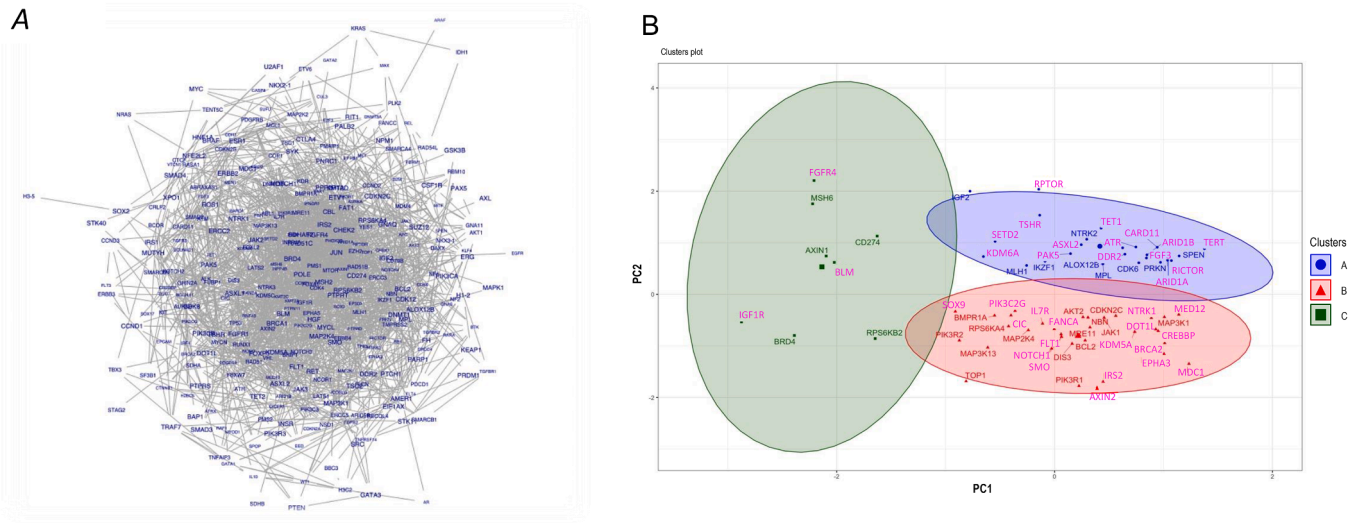

Fig. 2. Networks of mutated genes and K-Means clustering. (A) Gene network graphs from the cases' training set. Mutated genes are the nodes, while the lines are the edges denoting interactions. (B) Three clusters of mutated genes were defined in a principal component 1 (PC1) and PC2 biplot of network statistics for mutated genes defining the network. Data points represent PC scores. Within each cluster, only genes altered in more than five patients were assumed to describe a signature. Selected genes were colored in light magenta. Both mutations and CNAs as events were considered.

structure, we used PC1 and PC2 scores as inputs to the K-means clustering method. Indeed, PCA demonstrated PC1 to account for 64% of the dataset variance, while PC1 plus PC2 had a 0.882 (0.635 + 0.247) proportion of variance. Together, PC1 and PC2 explain approximately 90% of the data set.

Three clusters were arbitrarily defined based on the *elbow* criterion. Twenty-four altered genes made up "cluster A" (*MLH1, MPL, CDK6, FGF3, IKZF1, PRKN, RICTOR, ARID1A, SPEN, ARID1B, KDM6A, PAK5, ALOX12B, TERT, CARD11, ATR, DDR2, ASXL2, SETD2, NTRK2, TET1, TSHR, IGF2* and *RPTOR*), 33 defined the "cluster B" (*AXIN2, PIK3R1, IRS2, TOP1, MDC1, EPHA3, SMO, MAP3K13, BRCA2, DIS3, BCL2, PIK3R2, NOTCH1, FLT1, KDM5A, CREBBP, MAP2K4, DOT1L, FANCA, MRE11, RPS6KA4, IL7R, JAK1, MAP3K1, AKT2, NTRK1, NBN, CDKN2C, MED12, CIC, BMPR1A, PIK3C2G* and *SOX9*), while 8 were included in

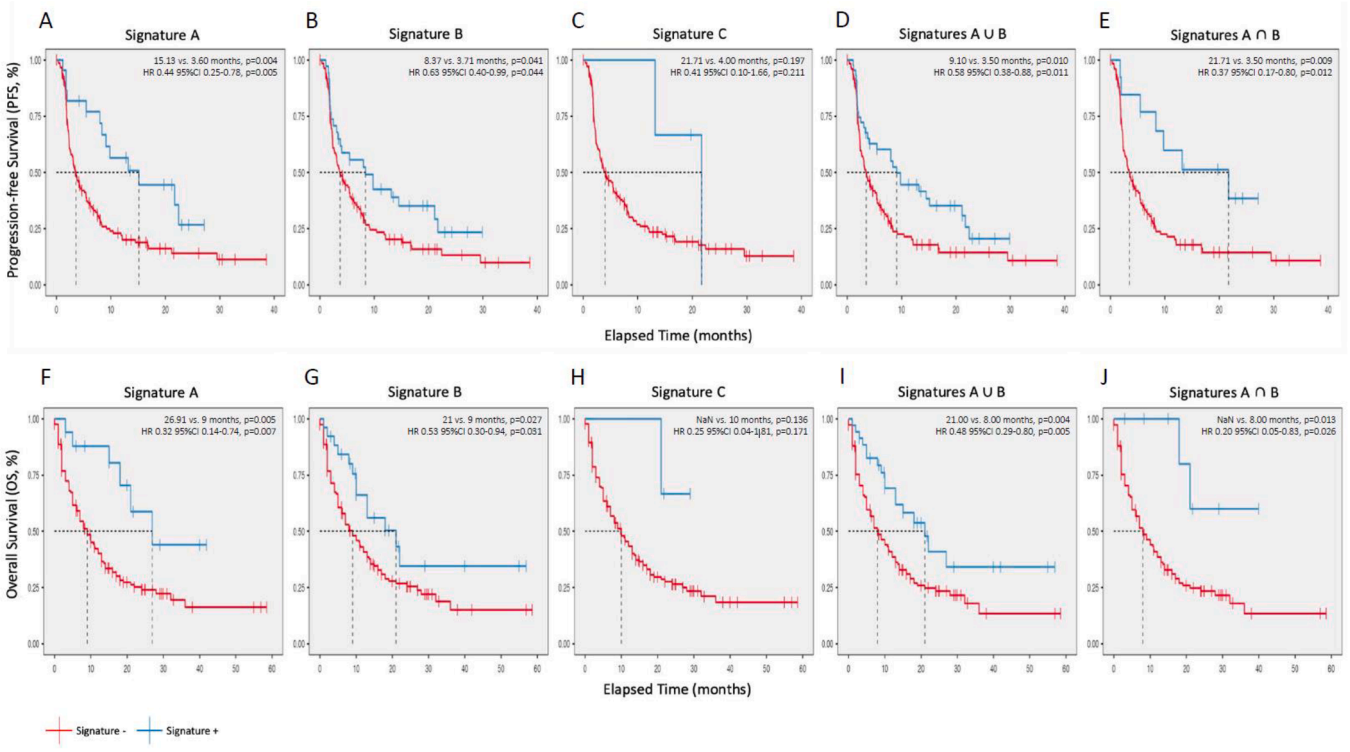

Fig. 3. Survival analysis for the cases training dataset. Kaplan-Meier curves of PFS with mutations in the set of genes of signature A (A), signature B (B), signature C (C), signature A ∪ B (D), and signature A ∩ B (E), evaluating 243 patients included in the training dataset. Kaplan-Meier curves of OS with mutations in the set of genes of signature A (F), signature B (G), signature C (H), signature A ∪ B (I), and signature A ∩ B (J), evaluating 243 patients included in the training dataset. A ∪ B-positive patients had at least two mutated genes from signature A OR at least two mutated genes from signature B. A ∩ B-positive patients had at least two mutated genes from signature A AND at least two mutated genes from signature B.

"cluster C" (*RPS6KB2, BRD4, IGF1R, BLM, AXIN1, CD274, MSH6* and *FGFR4*). However, only genes altered in more than five patients were assumed to describe a signature. Fifteen out of 24 genes were more likely to describe "signature A" (*FGF3, RICTOR, ARID1A, ARID1B, KDM6A, PAK5, TERT, CARD11, ATR, DDR2, ASXL2, SETD2, TET1, TSHR,* and *RPTOR*), 18 out of 33 were more likely to describe "signature B" (*AXIN2, IRS2, MDC1, EPHA3, SMO, BRCA2, NOTCH1, FLT1, KDM5A, CREBBP, DOT1L, FANCA, IL7R, NTRK1, MED12, CIC, PIK3C2G* and *SOX9*), while only 3 out of 8 genes were selected to characterize "signature C" (*IGF1R, BLM* and *FGFR4*) (Fig. 2B).

Patients with at least two mutated genes from signature A had a better median PFS than those with < 2 mutated genes (15.13 vs. 3.6 months, p = 0.004; Fig. 3A). Patients with at least two mutated genes from signature A had a better median PFS than those with < 2 mutated genes (8.37 vs. 3.71 months, p = 0.041; Fig. 3B). Also, if a patient had one mutated gene from signature A and one from signature B, he was considered neither A-positive nor B-positive: comprehensively "A or B" (A ∪ B) positive patients showed an increase in median PFS (9.10 vs. 3.50 months, p = 0.010), which was even more for patients positive to both signatures "A and B" (A ∩ B) (21.71 vs. 3.50 months, p = 0.009) (Fig. 3D-E). Nothing significant emerged for signature C (Fig. 3C). A ∪ B positive patients also had a better median OS of 21 vs. 8 months (p = 0.004). The OS median value was not even reached for those A ∩ B positives (p = 0.013) (Fig. 3F-J).

To test the results from the training model, an independent dataset of comparable cases was used. Independent survival analyses for the cases' test set confirmed the predictive value of the A ∪ B signature. When signatures were assessed together, patients with at least two mutated genes from signature A or at least two mutated genes from signature B showed longer PFS (10.39 vs. 4.13 months, p = 0.007) and OS (not reached vs. 13 months, p = 0.049) (Fig. 4A and C). Increments were also for patients who tested positive for both signatures A ∩ B (Fig. 4B and D). None of the patients in the test set harbored ≥ 2 mutated genes of the signature C.

Finally, cases from the training and test sets were gathered: univariate and multivariate analyses confirmed the A ∪ B signature as an independent predictive factor (PFS HR 0.58, 95% CI 0.43–0.77 and p < 0.001 for univariate analysis, PFS HR 0.58, 95% CI 0.36–0.93 and p = 0.024 for multivariate analysis; OS HR 0.52, 95% CI 0.35–0.77 and p = 0.001 for univariate analysis, OS HR 0.53, 95% CI 0.29–0.97 and p = 0.039 for multivariate analysis) (Supplementary Table 1). Conversely, although the A ∩ B signature predicted a reduced risk of disease progression (HR 0.46, 95% CI 0.27–0.77, p = 0.004) and death (HR 0.27, 95% CI 0.11–0.66, p = 0.004), the multivariate Cox regression model did not ensure it (Supplementary Table 2).

As expected, the A ∪ B signature had longer-lasting clinical benefits for first-line ICIs patients (10.39 vs. 5.42, p = 0.004) than for those receiving second (or subsequent) immunotherapy lines (5.47 vs. 2.70, p = 0.017) (Fig. 5A). And so was the A ∩ B signature (23 vs. 5.42, p = 0.012 in patients treated with first-line immunotherapy; 8.37 vs. 2.70, p = 0.05 in patients who received ICIs as subsequent-line of therapy) (Fig. 5B). While A or B positive patients were about 40% of those with DCB, 82.6% of cases with no-DCB harbored neither signature A nor B (χ^2 = 35.6, p < 0.001; Fig. 5C). Among DCB patients, 16% had at least two mutated genes of signature A and at least two mutated genes of signature B (A ∩ B). Also, 21.2% of them received first-line immunotherapy, while 16.9% received subsequent-line of ICIs. Of patients with no-DCB, 23.3% were immediately treated with immunotherapy, while 59.3% received it subsequently. Similarly, signatures proved to work better in patients receiving anti-PD-1 plus anti-CTLA-4 (Fig. 5D-F).

Notably, positivity to A or B signatures not only bridged the clinical benefit gap for patients undergoing subsequent-line immunotherapy or not receiving combined ICIs, but also improved outcomes. However, this was not the case for a separate TCGA [24] control group of 159 chemonaïve advanced NSCLCs (Table 1). They all underwent WES and mainly received doublets regimens with one of the platins and one of the third-

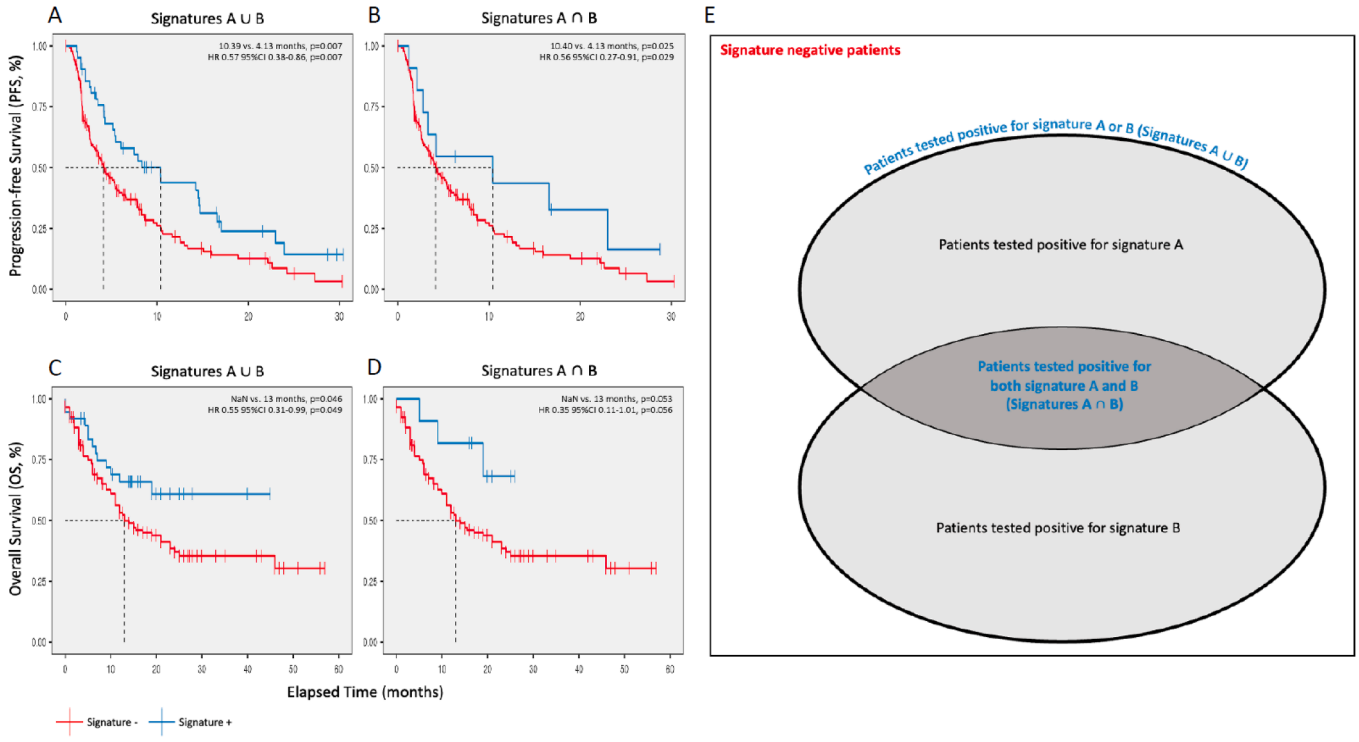

Fig. 4. Survival analysis for the cases test dataset. Kaplan-Meier curves of PFS with mutations in the set of genes of signature A ∪ B (A) and signature A ∩ B (B) evaluating 242 patients included in the test dataset. Kaplan-Meier curves of OS with mutations in the set of genes of signature A ∪ B (C) and signature A ∩ B (D) evaluating 242 patients included in the test dataset. (E) Venn diagram of patients clustering according to the harboring signatures. A ∪ B-positive patients had at least two mutated genes from signature A OR at least two mutated genes from signature B. A ∩ B-positive patients had at least two mutated genes from signature A AND at least two mutated genes from signature B.

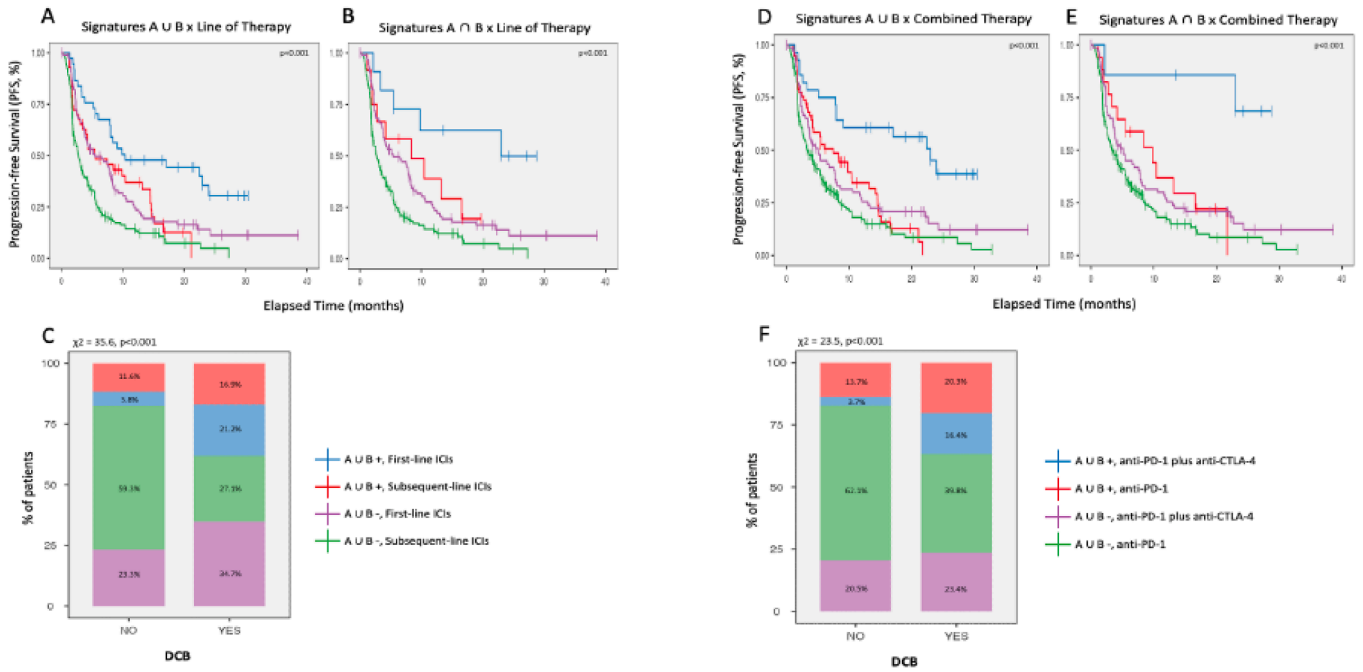

Fig. 5. Signature-related survival analysis. Kaplan-Meier curves of PFS with mutations in the set of genes of signature A ∪ B (A) and signature A ∩ B (B) evaluating the 485 cases who received ICI as first or subsequent-line of therapy. (C) Stacked bar plots showing the percentage of patients having durable clinical benefit with respect to A ∪ B signature positivity and line of immunotherapy. Kaplan-Meier curves of PFS with mutations in the set of genes of signature A ∪ B (D) and signature A ∩ B (E) evaluating the 485 cases who received ICI as mono- (anti-PD-1 only) or combined therapy (anti-PD-1 plus anti-CTLA-4). (F) Stacked bar plots showing the percentage of patients having durable clinical benefit with respect to A ∪ B signature positivity and immunotherapy combination.

generation chemotherapy agents [40,41]. For them, survival analyses showed no PFS benefit for signature A (HR 1.07, 95% CI 0.71–1.61, $p = 0.753$), B (HR 0.72, 95% CI 0.47–1.08, $p = 0.112$), A ∪ B (HR 0.99 95% CI, 0.67–1.45, $p = 0.952$) and A ∩ B (HR 0.72, 95% CI 0.41–1.29, $p = 0.274$). Nothing emerged concerning OS either (HR 0.95, 95% CI 0.61–1.48 and $p = 0.824$ for signature A; HR 0.76, 95% CI 0.50–1.17 and $p = 0.11$ for signature B; HR 0.89, 95% CI 0.59–1.33 and $p = 0.566$ for A ∪ B; HR 0.73, 95% CI 0.40–1.32 and $p = 0.297$ for A ∩ B).

Two hundreds and seventy-seven different mutations were identified among 15 genes defining the signature A, 64 of which were known disease drivers (Supplementary Table 3). Most resulted in a loss-of-function (LoF), except for the DDR2 amplification and the TERT promoter mutation, for which a gain-of-function (GoF) was recognized. Similarly, 347 different mutations were found in the 18 genes describing the signature B, including 33 known disease drivers (Supplementary Table 4). Again, these were mostly LoF mutations, except for the GoF NTRK1 amplification. Some of the driver mutations found in genes including *NOTCH* (F853C/I), *IL7R* (I241M), and *EPHA3* (C202_P203delins *) do not yet have a known biological effect.

ShinyGO analyses revealed significant involvement of signature A-related genes *ARID1A, ARID1B, KDM6A*, and *SETD2* in nucleosome remodelling (Fold Enrichment 21.107, Enrichment adjusted $p = 0.002$). Remodelling was mainly related to the SWI/SNF family of the ATP-dependent chromatin remodelling complex (including *ARID1A* and *ARID1B*; Fold Enrichment 607.893, Enrichment adjusted $p < 0.001$) and the ATM-dependent pathway (involving *KDM6A* and *SETD2*; Fold Enrichment 253.289, Enrichment adjusted $p = 0.002$). Similarly, altered expression of the signature A-related genes *RICTOR, RPTOR, CARD11, DDR2, FGF3, TERT, TET1*, and *TSH3* were proved to affect cell survival and proliferation (Fold Enrichment 11,668, Enrichment adjusted $p < 0.001$). Survival and proliferation were guaranteed through the activation of the TOR signalling (involving *RICTOR, RPTOR, CARD11*, and *FGF3* mutations; Fold Enrichment 37.067, Enrichment adjusted $p < 0.001$). Negative regulation of the gene silencing (involving *TERT* and *TET1*; Fold Enrichment 84.429, Enrichment adjusted $p = 0.007$) and the extrinsic apoptotic signalling pathway (involving *TERT* and *PAK5*; Fold Enrichment 25.329, Enrichment adjusted $p = 0.04$) contributed to survival and proliferation, as well. ShinyGO pathway analyses also disclosed the significant involvement of signature B-related genes. *CREBBP, NOTCH1, SOX9, MED12, SMO, NTRK1, IRS2, IL7R, FLT1*, and *AXIN2* controlled cell number homeostasis (Fold Enrichment 10.307, Enrichment adjusted $p < 0.001$) via evolutionarily conserved cell-to-cell signalling pathways including NOTCH pathway (involving *CREBBP, NOTCH1, SOX9*, and *MED12*; Fold Enrichment 29.682, Enrichment adjusted $p = 0.004$) and the IL7-mediated FoxO pathway (involving *CREBBP, IRS2*, and *IL7R*; Fold Enrichment 84.429, Enrichment adjusted $p = 0.005$). The role of *NOTCH1, SMO, NTRK1, PIK3C2G, FLT1, IRS2*, and *EPHA3* in chemotaxis was also noted (Fold Enrichment 12,682, Enrichment adjusted $p < 0.001$). *CREBBP* and *SMO* have critical positions in the hedgehog signalling (Fold Enrichment 148.993, Enrichment adjusted $p = 0.004$), while *NTRK1, FLT1, SOX9, IRS2*, and *IL7R* appear to be necessary for the PI3K-Akt pathway activation (Fold Enrichment 51.692, Enrichment adjusted $p < 0.001$).

Through GSEA, was also found A ∪ B signature to significantly correlate (false discovery rate $q < 0.05$) with the epithelium-mesenchymal transition (EMT) and the inflammatory response. Expressly, signature-positive cell lines showed enriched expression of genes usually up-regulated by α and γ interferon proteins, *TNF-α* (via NF-kB), *TGF-β*, and *IL6* (via STAT3). Angiogenesis was also promoted. Conversely, the A ∪ B altered cell lines also exhibited reduced expression of genes handling oxidative phosphorylation and unfolded protein response. GSEA results are summarized in Supplementary Table 5 and Supplementary Figure 6.

4. Discussion

Large-scale evidence of non-random mutation patterns indicates dependency networks (i.e., epistatic relationships) between genes in multi-steps carcinogenesis [42–44]. While synergistic alterations often occur together to collaborate, antagonistic or functionally redundant

events are likely mutually exclusive [42,43]. For example, KEAP1 and TP53 mutations - which frequently co-occur - proved to promote collaborative cancer-related pathways in response to oxidative stress [45]. Conversely, mutations in *EGFR, KRAS*, and *BRAF* genes - involved in the same *MAPK* signaling pathway - may be redundant and are not usually observed in the same tumor [43]. Dependency networks are explored with network analysis. Although this approach has its roots in sociology and computer science [46], it can also describe, explore, and understand the connection of somatic variants (whether *drivers* or *passengers*) in cancer. The analysis is both a methodological tool and a theoretical paradigm aiding in integrating multi-omics data and inferring the tumor's biological underpinning. Dependency networks have been studied primarily in microbial ecosystems, where environmental forces select concomitant or mutually exclusive growing microorganisms [47,48]. Similarly, tumor microenvironment (TME) hypoxia, acidosis, competition for space and resources, and predation by the immune system could exert selective pressure and are necessary to define the compendium of genes cancer-related alterations [49]. In addition, selective pressure imposed by previous anticancer treatments can substantially influence co-mutation patterns. These deterministic insights are consistent with the hypothesis that different relationships between mutated genes imply diverse functional cooperation, leading to divergent clinical behaviors and variable sensitivity to therapy [43]. Based on the assumption that co-dependent alterations influence each other's probability of co-existing, measures of the connectedness of each pro-tumorigenic alteration (Degree, Betweenness, Closeness, Eigen Centrality, and Bonacich Power [30]) were used to reveal that some act like hubs in their molecular networks and can co-drive receptivity to immunotherapies. An artificial intelligence (AI)-based pattern recognition task clustered them into two main groups. The presence of at least two mutations in the coding sequence of *FGF3, RICTOR, ARID1A, ARID1B, KDM6A, PAK5, TERT, CARD11, ATR, DDR2, ASXL2, SETD2, TET1, TSHR, and RPTOR* (signature A) and/or the presence of at least two mutations in the coding sequence of *AXIN2, IRS2, MDC1, EPHA3, SMO, BRCA2, NOTCH1, FLT1, KDM5A, CREBBP, DOT1L, FANCA, IL7R, NTRK1, MED12, CIC, PIK3C2G* and *SOX9* (signature B), have positive predictive values in advanced NSCLCs undergoing ICIs. Predictivity of signatures was confirmed in an independent cohort of comparable patients. By contrast, no survival benefits were observed in a matched control group of advanced NSCLCs receiving standard chemotherapy. Signatures performed best 1) when combined, 2) for patients undergoing first-line immunotherapy, 3) and for those receiving combined ICIs. Immunotherapy has been changing the paradigm of NSCLC treatment in different settings and improved patients quality of life. However, only about 20% of unselected patients respond to these treatments [1–7] and the availability of predictive biomarkers is still an important need. While driver mutations in *EGFR, BRAF, ALK*, and *HER2* dictate the choice of target-specific therapy, the same cannot be attributed to PD-L1 and/or TMB because they are dynamic, inducible, and disease-dependent [50].

PD-L1 and TMB are continuous variables with no apparent upper limit to the relationship between increased marker levels and the degree of clinical benefit derived from the intervention [51]. Conversely, the biomarker's binary signaling of positivity or negativity excludes threshold problems [51]: somatic alterations are present or not. As a result, mutation-based signatures appear more stable, and the classifications designed on them may be more reproducible.

No correlation emerged between the signatures and PD-L1 expression. However, ICI administration in treatment-naïve patients with advanced NSCLC and A ∪ B signature positivity was associated with higher PFS (10.39 vs. 5.42 months), agreeing with the KeyNote 024 study [52] that used pembrolizumab in advanced NSCLC with PD-L1 > 50% (10.3 vs. 6.7 months). This clinical benefit was not achieved in PD-L1 positive patients enrolled in the IMpower 110 [6] and CheckMate 026 [4] studies. While Spigel and colleagues [6] found 8.1 vs. 5.0 months of median PFS in patients treated with atezolizumab compared to those receiving chemotherapy, the median PFS in the nivolumab group of CheckMate 026 [4] was 4.2 months versus 5.9 months in favor of platinum-based therapy. A ∪ B positive patients undergoing anti-PD-1 plus anti-CTLA-4 also showed higher PFS than A ∪ B negatives (23 vs. 5.09 months). Results were even better than CheckMate 227 [53], where the therapeutic strategy of combining nivolumab plus ipilimumab in advanced NSCLC and TMB ≥ 10 Mut/Mb resulted in a median PFS of 7.2 vs. 5.5 months compared to those underwent chemotherapy only. As expected, benefits were higher in patients who were positive to both signature A and B (A ∩ B).

Moreover, from a mechanistic point of view, the risks of assuming that non-synonymous mutations (TMB) or even PD-L1 expression led to ICI sensitivity are high. TMB is a biomarker that reflects the generic processes involved in initiating immune reactivity; it is generic (non-checkpoint-specific factor) and of little service in predicting immune-related therapies effectiveness [51]. On the other end, the PD-L1 predictive biomarker is related to the final effector phases of the immune cascade and is relevant only for specific conditions [51]. However, between TMB-h and high PD-L1 expression, two other events must occur: non-synonymous mutations should be translated into neoantigens and presented to the host immune system via MHC class I; the TME should offer pro-inflammatory traits. TME context is paramount when evaluating the efficacy of immunotherapy [51]. To reduce risks by assuming PD-L1 upregulation as tumor dependence on the PD-1/PD-L1 axis to evade an antitumor initiated and primed immune response, the combination of assessments of PD-L1 expression levels with phenotypic features of the tumor immune microenvironment is being actively explored. The suggested signatures are ideally suited to these circumstances.

Indeed, signature B-related genes (*CREBBP, NOTCH1, SOX9, MED12, SMO, NTRK1, IRS2, IL7R, FLT1*, and *AXIN2*) emerge to retain cell number homeostasis through evolutionarily conserved cell–cell signaling pathways. Cell-to-cell crosstalk is critical in allowing tumor cells to co-opt and modulate stromal and immune cells. Functional crosstalk between tumor and surrounding cells promotes pre-metastatic niche formation, neovascularization, and immune suppression [54]. More interestingly, pathway analysis revealed that the signature A-related genes (*ARID1A, ARID1B, KDM6A*, and *SETD2*) belong to the mammalian switch/sucrose non-fermentable (SWI/SNF) family affecting chromatin remodeling. Four different complexes use the energy of ATP hydrolysis to regulate DNA accessibility in vital cellular processes (including transcription, DNA repair, and replication). They are the imitation switch (ISWI) family, the chromodomain helicase DNA-binding (CHD) family, the INO80 family, and the SWI/SNF family [55]). Nevertheless, interestingly mutations in the SWI/SNF family-associated genes are the most frequent after genome doubling in lung cancers [56,57]. These mutations may remove tissue-specific constraints on the cancer genome and provide advantages to emerging subclones later in evolution [56].

Growing evidence reports that mutations in SWI/SNF components underlie tumorigenesis and drug sensitivity [57–59], such as the paradigmatic ones affecting *ARID1A*, which is a key member of the SWI/SNF family that serves histone methylation in somatic cells [60]. Respective LoF mutations occur in 5%-11% of lung cancers [61] and correlate positively with enhanced antitumor immunity in both preclinical [62,63] and clinical models [64]. *ARID1A* deficiency contributes to the high microsatellite instability and TMB, and modulates the immune microenvironment by promoting the PD-L1 expression [63]. Therefore, *ARID1A* deficiency tumors should be sensitized to anti-PD-L1 treatment [64]. Our previous findings concur with this view, confirming the role of *ARID1A* in promoting the hyper-mutated cancer phenotype and thus its immunogenicity [50]. Additionally, aberrations in *ARID1A* and other commonly mutated genes (e.g., *KDM6A* and *SETD2*) proved to regulate chromatin accessibility to IFN- and IL6-responsive genes and to associate with high upstream expression of IFNs and IL6 pathways [65–68]. The result is increased trafficking of cytokines, including TNF-α and TGF-β. In the presence of TNF-α, TGF-β may synergistically promote

inflammation [69]. IL6 is another major pro-inflammatory cytokine that blocks TGF-β-induced Treg differentiation [70,71], and in presence of TGF-β, it can polarize tumor-infiltrated CD4 + T cells towards Th17 [72]. Inflammatory signals induced in the tumor milieu regulate the functional fate of Th17 cells. On the one hand, they play a pro-cancer role by promoting angiogenesis and STAT3 oncogenic signaling [73]. On the other, they foster anticancer immunity both through direct IFN-γ production and by recruiting dendritic cells (DCs), natural killer cells (NKs), and CD8 + cytotoxic T lymphocytes (CTLs) in the TME [73].

Consistent with the above results, the present work demonstrated that signature-positive cell lines exhibit enriched expression of genes usually up-regulated by INF-α and IFN-γ proteins, IL6 (via STAT3), TNF-α (via NF-kB), and TGF-β. In addition, angiogenesis and EMT were also promoted.

During EMT, cancer cells lose their epithelial characteristics and acquire mesenchymal traits. This phenotypic switch often involves the upregulation of cell surface antigens targeted by immunotherapy, such as PD-L1 [74–76]. In addition, EMT can lead to the loss of major histocompatibility complex (MHC) molecules and antigen presentation machinery contributing to the immunotherapy resistance [77,78]. This impairment in antigen presentation can hinder the recognition of tumor cells by cytotoxic T lymphocytes (CTLs) and natural killer (NK) cells, which are crucial for eliminating cancer cells [79]. All these factors contribute to the formation of an immunosuppressive tumor microenvironment, compromising the efficacy of immunotherapy by inhibiting immune cell activation and effector functions.

On the contrary, A ∪ B altered cell lines exhibited reduced expression of genes handling oxidative phosphorylation (preferring aerobic glycolysis due to the Warburg effect [80]) and reduced response to unfolded proteins (which would be a pro-survival adaptive mechanism triggered by the accumulation of unfolded or misfolded proteins in the endoplasmic reticulum [81]).

The retrospective nature of the present study and the relatively small sample size are major limitations of the analysis. However, a proper statistical approach was used to avoid type 1 errors and minimize selection bias. Early-stage, surgically resected, and locally advanced tumors pretreated with radiotherapy were excluded. The reason is that several distinct co-mutations patterns are enriched in the late-stage disease, likely reflecting the acquisition of traits promoting tumor progression and metastatic dissemination. Further, since selective pressure imposed by previous anticancer therapy and combination treatments can substantially influence the patterns of co-mutations, a stratified analysis was conducted considering the line of therapy and the therapy combination.

The restriction of the present analysis to the 341 genes included in the MSK-IMPACT panel is a strength of the study. This smaller gene dataset increased the power to identify significantly different networks focusing on genes known to be necessary for cancer growth.

In conclusion, the present study suggests a dependency between mutated genes and a peculiar profile of mutations in late-stage NSCLCs with immune sensitivity. The hypothesis is that somatic LoF mutations in SWI/SNF-related genes and impaired cell-to-cell crosstalk may result in dysfunctional immune evasion and persistent buffering of pro-inflammatory cytokines across the TME. This “inflamed milieu” could affect TILs activity once immune checkpoint blockers are inhibited. Therefore, the signatures underlying these abnormalities could represent a clinically relevant readout and provide a suitable biomarker to improve the selection of patients who benefit from immunotherapy, with possibly important implications for personalized therapeutic decisions.

CRediT authorship contribution statement

Federico Cucchiara: Conceptualization, Methodology, Investigation, Data curation, Writing – original draft. **Stefania Crucitta:** Writing – review & editing. **Iacopo Petrini:** Supervision, Writing – review & editing. **Diego de Miguel Perez:** Writing – review & editing. **Martina Ruglioni:** Writing – review & editing. **Eleonora Pardini:** Writing – review & editing. **Christian Rolfo:** Conceptualization, Supervision, Writing – review & editing. **Romano Danesi:** Conceptualization, Supervision, Writing – review & editing. **Marzia Del Re:** Conceptualization, Supervision, Writing – review & editing.

Declaration of Competing Interest

The authors declare that they have no known competing financial interests or personal relationships that could have appeared to influence the work reported in this paper.

Acknowledgments

This research was partially funded under grants n. 2017NRW5K (PRIN 2017) and n. 20209KY3Y7 (PRIN 2020) from Ministero dell’Istruzione, dell’Università e della Ricerca (MIUR), Italy.

Appendix A. Supplementary data

Supplementary data to this article can be found online at https://doi.org/10.1016/j.lungcan.2023.107308.

References

[1] M. Reck, D. Rodríguez-Abreu, A.G. Robinson, R. Hui, T. Csőszi, A. Fülöp, M. Gottfried, N. Peled, A. Tafreshi, S. Cuffe, M. O’Brien, S. Rao, K. Hotta, M. A. Leiby, G.M. Lubiniecki, Y. Shentu, R. Rangwala, J.R. Brahmer, Pembrolizumab versus Chemotherapy for PD-L1–Positive Non–Small-Cell Lung Cancer, N. Engl. J. Med. 375 (19) (2016) 1823–1833.

[2] R.S. Herbst, P. Baas, D.-W. Kim, E. Felip, J.L. Pérez-Gracia, J.-Y. Han, J. Molina, J.-H. Kim, C.D. Arvis, M.-J. Ahn, M. Majem, M.J. Fidler, G. de Castro, M. Garrido, G. M. Lubiniecki, Y. Shentu, E. Im, M. Dolled-Filhart, E.B. Garon, Pembrolizumab versus docetaxel for previously treated, PD-L1-positive, advanced non-small-cell lung cancer (KEYNOTE-010): a randomised controlled trial, Lancet 387 (10027) (2016) 1540–1550.

[3] L. Horn, D.R. Spigel, E.E. Vokes, E. Holgado, N. Ready, M. Steins, E. Poddubskaya, H. Borghaei, E. Felip, L. Paz-Ares, A. Pluzanski, K.L. Reckamp, M.A. Burgio, M. Kohlhaeufl, D. Waterhouse, F. Barlesi, S. Antonia, O. Arrieta, J. Fayette, L. Crino, N. Rizvi, M. Reck, M.D. Hellmann, W.J. Geese, A. Li, A. Blackwood-Chirchir, D. Healey, J. Brahmer, W.E.E. Eberhardt, Nivolumab Versus Docetaxel in Previously Treated Patients With Advanced Non-Small-Cell Lung Cancer: Two-Year Outcomes From Two Randomized, Open-Label, Phase III Trials (CheckMate 017 and CheckMate 057), J. Clin. Oncol. 35 (35) (2017) 3924–3933, https://doi.org/10.1200/JCO.2017.74.3062.

[4] D.P. Carbone, M. Reck, L. Paz-Ares, B. Creelan, L. Horn, M. Steins, E. Felip, M. M. van den Heuvel, T.-E. Ciuleanu, F. Badin, N. Ready, T.J.N. Hiltermann, S. Nair, R. Juergens, S. Peters, E. Minenza, J.M. Wrangle, D. Rodriguez-Abreu, H. Borghaei, G.R. Blumenschein, L.C. Villaruz, L. Havel, J. Krejci, J. Corral Jaime, H. Chang, W. J. Geese, P. Bhagavatheeswaran, A.C. Chen, M.A. Socinski, First-Line Nivolumab in Stage IV or Recurrent Non–Small-Cell Lung Cancer, N. Engl. J. Med. 376 (25) (2017) 2415–2426.

[5] A. Rittmeyer, F. Barlesi, D. Waterkamp, K. Park, F. Ciardiello, J. von Pawel, S. M. Gadgeel, T. Hida, D.M. Kowalski, M.C. Dols, D.L. Cortinovis, J. Leach, J. Polikoff, C. Barrios, F. Kabbinavar, O.A. Frontera, F. De Marinis, H. Turna, J.-S. Lee, M. Ballinger, M. Kowanetz, P. He, D.S. Chen, A. Sandler, D.R. Gandara, Atezolizumab versus docetaxel in patients with previously treated non-small-cell lung cancer (OAK): a phase 3, open-label, multicentre randomised controlled trial, Lancet 389 (10066) (2017) 255–265.

[6] R.S. Herbst, G. Giaccone, F. de Marinis, N. Reinmuth, A. Vergnenegre, C.H. Barrios, M. Morise, E. Felip, Z. Andric, S. Geater, M. Ozguroglu, W. Zou, A. Sandler, I. Enquist, K. Komatsubara, Y. Deng, H. Kuriki, X. Wen, M. McCleland, S. Mocci, J. Jassem, D.R. Spigel, Atezolizumab for First-Line Treatment of PD-L1-Selected Patients with NSCLC, N. Engl. J. Med. 383 (14) (2020) 1328–1339, https://doi.org/10.1056/NEJMoa1917346.

[7] S.J. Antonia, A. Villegas, D. Daniel, D. Vicente, S. Murakami, R. Hui, T. Yokoi, A. Chiappori, K.H. Lee, M. de Wit, B.C. Cho, M. Bourhaba, X. Quantin, T. Tokito, T. Mekhail, D. Planchard, Y.-C. Kim, C.S. Karapetis, S. Hiret, G. Ostoros, K. Kubota, J.E. Gray, L. Paz-Ares, J. de Castro Carpeño, C. Wadsworth, G. Melillo, H. Jiang, Y. Huang, P.A. Dennis, M. Özgüroğlu, Durvalumab after Chemoradiotherapy in Stage III Non–Small-Cell Lung Cancer, N. Engl. J. Med. 377 (20) (2017) 1919–1929.

[8] E.E. Vokes, N. Ready, E. Felip, L. Horn, M.A. Burgio, S.J. Antonia, O. Arén Frontera, S. Gettinger, E. Holgado, D. Spigel, D. Waterhouse, M. Domine, M. Garassino, L.Q. M. Chow, G. Blumenschein, F. Barlesi, B. Coudert, J. Gainor, O. Arrieta, J. Brahmer, C. Butts, M. Steins, W.J. Geese, A. Li, D. Healey, L. Crinò, Nivolumab versus docetaxel in previously treated advanced non-small-cell lung cancer

(CheckMate 017 and CheckMate 057): 3-year update and outcomes in patients with liver metastases, Ann. Oncol. 29 (4) (2018) 959–965.
[9] A.M. Hopkins, A. Rowland, G. Kichenadasse, M.D. Wiese, H. Gurney, R. A. McKinnon, C.S. Karapetis, M.J. Sorich, Predicting response and toxicity to immune checkpoint inhibitors using routinely available blood and clinical markers, Br. J. Cancer 117 (7) (2017) 913–920, https://doi.org/10.1038/bjc.2017.274.
[10] T.A. Chan, M. Yarchoan, E. Jaffee, C. Swanton, S.A. Quezada, A. Stenzinger, S. Peters, Development of tumor mutation burden as an immunotherapy biomarker: utility for the oncology clinic, Ann. Oncol. 30 (1) (2019) 44–56, https://doi.org/10.1093/annonc/mdy495.
[11] A. Addeo, A. Friedlaender, G.L. Banna, G.J. Weiss, TMB or not TMB as a biomarker: That is the question, Crit. Rev. Oncol. Hematol. 163 (2021), 103374, https://doi.org/10.1016/j.critrevonc.2021.103374.
[12] K. Schwarze, J. Buchanan, J.C. Taylor, S. Wordsworth, Are whole-exome and whole-genome sequencing approaches cost-effective? A systematic review of the literature, Genet. Med. 20 (10) (2018) 1122–1130, https://doi.org/10.1038/gim.2017.247.
[13] A.M. Goodman, S. Kato, L. Bazhenova, S.P. Patel, G.M. Frampton, V. Miller, P. J. Stephens, G.A. Daniels, R. Kurzrock, Tumor Mutational Burden as an Independent Predictor of Response to Immunotherapy in Diverse Cancers, Mol. Cancer Ther. 16 (11) (2017) 2598–2608.
[14] V. Subbiah, D.B. Solit, T.A. Chan, R. Kurzrock, The FDA approval of pembrolizumab for adult and pediatric patients with tumor mutational burden (TMB) >/=10: a decision centered on empowering patients and their physicians, Ann. Oncol. 31 (9) (2020) 1115–1118, https://doi.org/10.1016/j.annonc.2020.07.002.
[15] D. Kazdal, V. Endris, M. Allgauer, M. Kriegsmann, J. Leichsenring, A.L. Volckmar, A. Harms, M. Kirchner, K. Kriegsmann, O. Neumann, R. Brandt, S.B. Talla, E. Rempel, C. Ploeger, M. von Winterfeld, P. Christopoulos, D.M. Merino, M. Stewart, J. Allen, H. Bischoff, M. Meister, T. Muley, F. Herth, R. Penzel, A. Warth, H. Winter, S. Frohling, S. Peters, C. Swanton, M. Thomas, P. Schirmacher, J. Budczies, A. Stenzinger, Spatial and Temporal Heterogeneity of Panel-Based Tumor Mutational Burden in Pulmonary Adenocarcinoma: Separating Biology From Technical Artifacts, J. Thorac. Oncol. 14 (11) (2019) 1935–1947, https://doi.org/10.1016/j.jtho.2019.07.006.
[16] F. Cucchiara, I. Petrini, A. Passaro, I. Attili, S. Crucitta, E. Pardini, F. de Marinis, R. Danesi, M. Del Re, Gene network Analysis Defines a Subgroup of Small Cell Lung Cancer patients With Short Survival, Clin. Lung Cancer 23 (6) (2022) 510–521, https://doi.org/10.1016/j.cllc.2022.05.012.
[17] E. Cerami, J. Gao, U. Dogrusoz, B.E. Gross, S.O. Sumer, B.A. Aksoy, A. Jacobsen, C. J. Byrne, M.L. Heuer, E. Larsson, Y. Antipin, B. Reva, C. Sander, N. Schultz, The cBio cancer genomics portal: an open platform for exploring multidimensional cancer genomics data, Cancer Discov. 2 (5) (2012) 401–404.
[18] J. Gao, B.A. Aksoy, U. Dogrusoz, G. Dresdner, B. Gross, S.O. Sumer, Y. Sun, A. Jacobsen, R. Sinha, E. Larsson, E. Cerami, C. Sander, N. Schultz, Integrative analysis of complex cancer genomics and clinical profiles using the cBioPortal, Sci. Signal. 6 (269) (2013) pl1, https://doi.org/10.1126/scisignal.2004088.
[19] R.M. Samstein, C.H. Lee, A.N. Shoushtari, M.D. Hellmann, R. Shen, Y.Y. Janjigian, D.A. Barron, A. Zehir, E.J. Jordan, A. Omuro, T.J. Kaley, S.M. Kendall, R.J. Motzer, A.A. Hakimi, M.H. Voss, P. Russo, J. Rosenberg, G. Iyer, B.H. Bochner, D.F. Bajorin, H.A. Al-Ahmadie, J.E. Chaft, C.M. Rudin, G.J. Riely, S. Baxi, A.L. Ho, R.J. Wong, D. G. Pfister, J.D. Wolchok, C.A. Barker, P.H. Gutin, C.W. Brennan, V. Tabar, I. K. Mellinghoff, L.M. DeAngelis, C.E. Ariyan, N. Lee, W.D. Tap, M.M. Gounder, S. P. D'Angelo, L. Saltz, Z.K. Stadler, H.I. Scher, J. Baselga, P. Razavi, C.A. Klebanoff, R. Yaeger, N.H. Segal, G.Y. Ku, R.P. DeMatteo, M. Ladanyi, N.A. Rizvi, M.F. Berger, N. Riaz, D.B. Solit, T.A. Chan, L.G.T. Morris, Tumor mutational load predicts survival after immunotherapy across multiple cancer types, Nat. Genet. 51 (2) (2019) 202–206, https://doi.org/10.1038/s41588-018-0312-8.
[20] D. Miao, C.A. Margolis, N.I. Vokes, D. Liu, A. Taylor-Weiner, S.M. Wankowicz, D. Adeegbe, D. Keliher, B. Schilling, A. Tracy, M. Manos, N.G. Chau, G.J. Hanna, P. Polak, S.J. Rodig, S. Signoretti, L.M. Sholl, J.A. Engelman, G. Getz, P.A. Janne, R. I. Haddad, T.K. Choueiri, D.A. Barbie, R. Haq, M.M. Awad, D. Schadendorf, F. S. Hodi, J. Bellmunt, K.K. Wong, P. Hammerman, E.M. Van Allen, Genomic correlates of response to immune checkpoint blockade in microsatellite-stable solid tumors, Nat. Genet. 50 (9) (2018) 1271–1281, https://doi.org/10.1038/s41588-018-0200-2.
[21] N.A. Rizvi, M.D. Hellmann, A. Snyder, P. Kvistborg, V. Makarov, J.J. Havel, W. Lee, J. Yuan, P. Wong, T.S. Ho, M.L. Miller, N. Rekhtman, A.L. Moreira, F. Ibrahim, C. Bruggeman, B. Gasmi, R. Zappasodi, Y. Maeda, C. Sander, E.B. Garon, T. Merghoub, J.D. Wolchok, T.N. Schumacher, T.A. Chan, Mutational landscape determines sensitivity to PD-1 blockade in non–small cell lung cancer, Science 348 (6230) (2015) 124–128.
[22] H. Rizvi, F. Sanchez-Vega, K. La, W. Chatila, P. Jonsson, D. Halpenny, A. Plodkowski, N. Long, J.L. Sauter, N. Rekhtman, T. Hollmann, K.A. Schalper, J. F. Gainor, R. Shen, A. Ni, K.C. Arbour, T. Merghoub, J. Wolchok, A. Snyder, J. E. Chaft, M.G. Kris, C.M. Rudin, N.D. Socci, M.F. Berger, B.S. Taylor, A. Zehir, D. B. Solit, M.E. Arcila, M. Ladanyi, G.J. Riely, N. Schultz, M.D. Hellmann, Molecular Determinants of Response to Anti-Programmed Cell Death (PD)-1 and Anti-Programmed Death-Ligand 1 (PD-L1) Blockade in Patients With Non-Small-Cell Lung Cancer Profiled With Targeted Next-Generation Sequencing, J. Clin. Oncol. 36 (7) (2018) 633–641, https://doi.org/10.1200/JCO.2017.75.3384.
[23] M.D. Hellmann, T. Nathanson, H. Rizvi, B.C. Creelan, F. Sanchez-Vega, A. Ahuja, A. i. Ni, J.B. Novik, L.M.B. Mangarin, M. Abu-Akeel, C. Liu, J.L. Sauter, N. Rekhtman, E. Chang, M.K. Callahan, J.E. Chaft, M.H. Voss, M. Tenet, X.-M. Li, K. Covello, A. Renninger, P. Vitazka, W.J. Geese, H. Borghaei, C.M. Rudin, S.J. Antonia, C. Swanton, J. Hammerbacher, T. Merghoub, N. McGranahan, A. Snyder, J. D. Wolchok, Genomic Features of Response to Combination Immunotherapy in Patients with Advanced Non-Small-Cell Lung Cancer, Cancer Cell 33 (5) (2018) 843–852.e4.
[24] K. Tomczak, P. Czerwinska, M. Wiznerowicz, The Cancer Genome Atlas (TCGA): an immeasurable source of knowledge, Contemp Oncol (Pozn) 19 (1A) (2015) A68–A77, https://doi.org/10.5114/wo.2014.47136.
[25] N. Cancer Genome Atlas Research, Comprehensive molecular profiling of lung adenocarcinoma, Nature 511(7511) (2014) 543-50. doi:10.1038/nature13385.
[26] N. Cancer Genome Atlas Research, Comprehensive genomic characterization of squamous cell lung cancers, Nature 489(7417) (2012) 519-25. doi:10.1038/nature11404.
[27] A. Colaprico, T.C. Silva, C. Olsen, L. Garofano, C. Cava, D. Garolini, T.S. Sabedot, T. M. Malta, S.M. Pagnotta, I. Castiglioni, M. Ceccarelli, G. Bontempi, H. Noushmehr, TCGAbiolinks: an R/Bioconductor package for integrative analysis of TCGA data, Nucleic Acids Res. 44 (8) (2016) e71.
[28] A. Mayakonda, D.C. Lin, Y. Assenov, C. Plass, H.P. Koeffler, Maftools: efficient and comprehensive analysis of somatic variants in cancer, Genome Res. 28 (11) (2018) 1747–1756, https://doi.org/10.1101/gr.239244.118.
[29] G. Csardi, T. Nepusz, The Igraph Software Package for Complex Network Research, InterJournal, Complex Systems (2005) 1695.
[30] P. Bonacich, Power and Centrality: A Family of Measures, Am. J. Sociol. 92 (5) (1987) 1170–1182.
[31] D. Steinley, K-means clustering: a half-century synthesis, Br. J. Math. Stat. Psychol. 59 (Pt 1) (2006) 1–34, https://doi.org/10.1348/000711005X48266.
[32] I.T. Jolliffe, J. Cadima, Principal component analysis: a review and recent developments, Philos Trans A Math Phys Eng Sci 374 (2065) (2016) 20150202, https://doi.org/10.1098/rsta.2015.0202.
[33] L.L. Hsu, A.C. Culhane, Impact of Data Preprocessing on Integrative Matrix Factorization of Single Cell Data, Front. Oncol. 10 (2020) 973, https://doi.org/10.3389/fonc.2020.00973.
[34] M.E. Celebi, H.A. Kingravi, P.A. Vela, A comparative study of efficient initialization methods for the k-means clustering algorithm, Expert Syst. Appl. 40 (1) (2013) 200–210, https://doi.org/10.1016/j.eswa.2012.07.021.
[35] S. Lloyd, Least squares quantization in PCM, IEEE Trans. Inf. Theory 28 (2) (1982) 129–137, https://doi.org/10.1109/TIT.1982.1056489.
[36] M.A. Syakur, B.K. Khotimah, E.M.S. Rochman, B.D. Satoto, Integration K-Means Clustering Method and Elbow Method For Identification of The Best Customer Profile Cluster, IOP Conf. Ser.: Mater. Sci. Eng. 336 (1) (2018), 012017, https://doi.org/10.1088/1757-899X/336/1/012017.
[37] S.X. Ge, D. Jung, R. Yao, A. Valencia, ShinyGO: a graphical gene-set enrichment tool for animals and plants, Bioinformatics 36 (8) (2020) 2628–2629.
[38] A. Subramanian, P. Tamayo, V.K. Mootha, S. Mukherjee, B.L. Ebert, M.A. Gillette, A. Paulovich, S.L. Pomeroy, T.R. Golub, E.S. Lander, J.P. Mesirov, Gene set enrichment analysis: a knowledge-based approach for interpreting genome-wide expression profiles, PNAS 102 (43) (2005) 15545–15550, https://doi.org/10.1073/pnas.0506580102.
[39] A. Liberzon, C. Birger, H. Thorvaldsdottir, M. Ghandi, J.P. Mesirov, P. Tamayo, The Molecular Signatures Database (MSigDB) hallmark gene set collection, Cell Syst. 1 (6) (2015) 417–425, https://doi.org/10.1016/j.cels.2015.12.004.
[40] D.S. Ettinger, D.E. Wood, D.L. Aisner, W. Akerley, J.R. Bauman, A. Bharat, D.S. Bruno, J.Y. Chang, L.R. Chirieac, T.A. D'Amico, M. DeCamp, T.J. Dilling, J. Dowell, S. Gettinger, T.E. Grotz, M.A. Gubens, A. Hegde, R.P. Lackner, M. Lanuti, J. Lin, B. W. Loo, C.M. Lovly, F. Maldonado, E. Massarelli, D. Morgensztern, T. Ng, G.A. Otterson, J.M. Pacheco, S.P. Patel, G.J. Riely, J. Riess, S.E. Schild, T.A. Shapiro, A. P. Singh, J. Stevenson, A. Tam, T. Tanvetyanon, J. Yanagawa, S.C. Yang, E. Yau, K. Gregory, M. Hughes, Non-Small Cell Lung Cancer, Version 3.2022, NCCN Clinical Practice Guidelines in Oncology, J Natl Compr Canc Netw 20(5) (2022) 497-530. doi:10.6004/jnccn.2022.0025.
[41] D. Planchard, S. Popat, K. Kerr, S. Novello, E.F. Smit, C. Faivre-Finn, T.S. Mok, M. Reck, P.E. Van Schil, M.D. Hellmann, S. Peters, E.G. Committee, Metastatic non-small cell lung cancer: ESMO Clinical Practice Guidelines for diagnosis, treatment and follow-up, Ann Oncol 29(Suppl 4) (2018) iv192-iv237. doi:10.1093/annonc/mdy275.
[42] M. Mina, F. Raynaud, D. Tavernari, E. Battistello, S. Sungalee, S. Saghafinia, T. Laessle, F. Sanchez-Vega, N. Schultz, E. Oricchio, G. Ciriello, Conditional Selection of Genomic Alterations Dictates Cancer Evolution and Oncogenic Dependencies, Cancer Cell 32 (2) (2017) 155–168 e6, https://doi.org/10.1016/j.ccell.2017.06.010.
[43] F. Skoulidis, J.V. Heymach, Co-occurring genomic alterations in non-small-cell lung cancer biology and therapy, Nat. Rev. Cancer 19 (9) (2019) 495–509, https://doi.org/10.1038/s41568-019-0179-8.
[44] J. van de Haar, S. Canisius, M.K. Yu, E.E. Voest, L.F.A. Wessels, T. Ideker, Identifying Epistasis in Cancer Genomes: A Delicate Affair, Cell 177 (6) (2019) 1375–1383, https://doi.org/10.1016/j.cell.2019.05.005.
[45] M.M. Saleh, M. Scheffler, S. Merkelbach-Bruse, A.H. Scheel, B. Ulmer, J. Wolf, R. Buettner, Comprehensive Analysis of TP53 and KEAP1 Mutations and Their Impact on Survival in Localized- and Advanced-Stage NSCLC, J. Thorac. Oncol. 17 (1) (2022) 76–88, https://doi.org/10.1016/j.jtho.2021.08.764.
[46] D.A. Luke, J.K. Harris, Network analysis in public health: history, methods, and applications, Annu. Rev. Public Health 28 (2007) 69–93, https://doi.org/10.1146/annurev.publhealth.28.021406.144132.
[47] A.B.A. Shafer, J.B.W. Wolf, J. Wiens, Widespread evidence for incipient ecological speciation: a meta-analysis of isolation-by-ecology, Ecol. Lett. 16 (7) (2013) 940–950.

[48] K.A. Whittaker, T.A. Rynearson, Evidence for environmental and ecological selection in a microbe with no geographic limits to gene flow, PNAS 114 (10) (2017) 2651–2656, https://doi.org/10.1073/pnas.1612346114.
[49] S.C. Nunes, Tumor Microenvironment - Selective Pressures Boosting Cancer Progression, Adv. Exp. Med. Biol. 1219 (2020) 35–49, https://doi.org/10.1007/978-3-030-34025-4_2.
[50] M. Del Re, F. Cucchiara, E. Rofi, L. Fontanelli, I. Petrini, N. Gri, G. Pasquini, M. Rizzo, M. Gabelloni, L. Belluomini, S. Crucitta, R. Ciampi, A. Frassoldati, E. Neri, C. Porta, R. Danesi, A multiparametric approach to improve the prediction of response to immunotherapy in patients with metastatic NSCLC, Cancer Immunol. Immunother. 70 (6) (2021) 1667–1678, https://doi.org/10.1007/s00262-020-02810-6.
[51] D.R. Camidge, R.C. Doebele, K.M. Kerr, Comparing and contrasting predictive biomarkers for immunotherapy and targeted therapy of NSCLC, Nat. Rev. Clin. Oncol. 16 (6) (2019) 341–355, https://doi.org/10.1038/s41571-019-0173-9.
[52] M. Reck, D. Rodriguez-Abreu, A.G. Robinson, R. Hui, T. Csoszi, A. Fulop, M. Gottfried, N. Peled, A. Tafreshi, S. Cuffe, M. O'Brien, S. Rao, K. Hotta, K. Vandormael, A. Riccio, J. Yang, M.C. Pietanza, J.R. Brahmer, Updated Analysis of KEYNOTE-024: Pembrolizumab Versus Platinum-Based Chemotherapy for Advanced Non-Small-Cell Lung Cancer With PD-L1 Tumor Proportion Score of 50% or Greater, J. Clin. Oncol. 37 (7) (2019) 537–546, https://doi.org/10.1200/JCO.18.00149.
[53] M.D. Hellmann, L. Paz-Ares, R. Bernabe Caro, B. Zurawski, S.-W. Kim, E. Carcereny Costa, K. Park, A. Alexandru, L. Lupinacci, E. de la Mora Jimenez, H. Sakai, I. Albert, A. Vergnenegre, S. Peters, K. Syrigos, F. Barlesi, M. Reck, H. Borghaei, J. R. Brahmer, K.J. O'Byrne, W.J. Geese, P. Bhagavatheeswaran, S.K. Rabindran, R. S. Kasinathan, F.E. Nathan, S.S. Ramalingam, Nivolumab plus Ipilimumab in Advanced Non–Small-Cell Lung Cancer, N. Engl. J. Med. 381 (21) (2019) 2020–2031.
[54] C. Chiodoni, M.T. Di Martino, F. Zazzeroni, M. Caraglia, M. Donadelli, S. Meschini, C. Leonetti, K. Scotlandi, Cell communication and signaling: how to turn bad language into positive one, J. Exp. Clin. Cancer Res. 38 (1) (2019) 128, https://doi.org/10.1186/s13046-019-1122-2.
[55] C.R. Clapier, J. Iwasa, B.R. Cairns, C.L. Peterson, Mechanisms of action and regulation of ATP-dependent chromatin-remodelling complexes, Nat. Rev. Mol. Cell Biol. 18 (7) (2017) 407–422, https://doi.org/10.1038/nrm.2017.26.
[56] M. Jamal-Hanjani, G.A. Wilson, N. McGranahan, N.J. Birkbak, T.B.K. Watkins, S. Veeriah, S. Shafi, D.H. Johnson, R. Mitter, R. Rosenthal, M. Salm, S. Horswell, M. Escudero, N. Matthews, A. Rowan, T. Chambers, D.A. Moore, S. Turajlic, H. Xu, S.-M. Lee, M.D. Forster, T. Ahmad, C.T. Hiley, C. Abbosh, M. Falzon, E. Borg, T. Marafioti, D. Lawrence, M. Hayward, S. Kolvekar, N. Panagiotopoulos, S. M. Janes, R. Thakrar, A. Ahmed, F. Blackhall, Y. Summers, R. Shah, L. Joseph, A. M. Quinn, P.A. Crosbie, B. Naidu, G. Middleton, G. Langman, S. Trotter, M. Nicolson, H. Remmen, K. Kerr, M. Chetty, L. Gomersall, D.A. Fennell, A. Nakas, S. Rathinam, G. Anand, S. Khan, P. Russell, V. Ezhil, B. Ismail, M. Irvin-Sellers, V. Prakash, J.F. Lester, M. Kornaszewska, R. Attanoos, H. Adams, H. Davies, S. Dentro, P. Taniere, B. O'Sullivan, H.L. Lowe, J.A. Hartley, N. Iles, H. Bell, Y. Ngai, J.A. Shaw, J. Herrero, Z. Szallasi, R.F. Schwarz, A. Stewart, S.A. Quezada, J. Le Quesne, P. Van Loo, C. Dive, A. Hackshaw, C. Swanton, Tracking the Evolution of Non-Small-Cell Lung Cancer, N. Engl. J. Med. 376 (22) (2017) 2109–2121.
[57] P. Peinado, A. Andrades, M. Cuadros, M.I. Rodriguez, I.F. Coira, D.J. Garcia, J. C. Alvarez-Perez, C. Balinas-Gavira, A.M. Arenas, J.R. Patino-Mercau, J. Sanjuan-Hidalgo, O.A. Romero, L.M. Montuenga, J. Carretero, M. Sanchez-Cespedes, P. P. Medina, Comprehensive Analysis of SWI/SNF Inactivation in Lung Adenocarcinoma Cell Models, Cancers (Basel) 12 (12) (2020), https://doi.org/10.3390/cancers12123712.
[58] T. Fukumoto, E. Magno, R. Zhang, SWI/SNF Complexes in Ovarian Cancer: Mechanistic Insights and Therapeutic Implications, Mol. Cancer Res. 16 (12) (2018) 1819–1825.
[59] R.M. Chabanon, D. Morel, S. Postel-Vinay, Exploiting epigenetic vulnerabilities in solid tumors: Novel therapeutic opportunities in the treatment of SWI/SNF-defective cancers, Semin. Cancer Biol. 61 (2020) 180–198, https://doi.org/10.1016/j.semcancer.2019.09.018.
[60] T.W.R. Kelso, D.K. Porter, M.L. Amaral, M.N. Shokhirev, C. Benner, D. C. Hargreaves, Chromatin accessibility underlies synthetic lethality of SWI/SNF subunits in ARID1A-mutant cancers, Elife 6 (2017), https://doi.org/10.7554/eLife.30506.
[61] X. Liu, Z. Li, Z. Wang, F. Liu, L. Zhang, J. Ke, X.u. Xu, Y. Zhang, Y. Yuan, T. Wei, Q. Shan, Y. Chen, W. Huang, J. Gao, N. Wu, F. Chen, L. Sun, Z. Qiu, Y. Deng, X. Wang, Chromatin Remodeling Induced by ARID1A Loss in Lung Cancer Promotes Glycolysis and Confers JQ1 Vulnerability, Cancer Res. 82 (5) (2022) 791–804.
[62] S. Goswami, Y. Chen, S. Anandhan, P.M. Szabo, S. Basu, J.M. Blando, W. Liu, J. Zhang, S.M. Natarajan, L. Xiong, B. Guan, S.S. Yadav, A. Saci, J.P. Allison, M. D. Galsky, P. Sharma, ARID1A mutation plus CXCL13 expression act as combinatorial biomarkers to predict responses to immune checkpoint therapy in mUCC, Sci. Transl. Med. 12 (548) (2020), https://doi.org/10.1126/scitranslmed.abc4220.
[63] G. Hu, W. Tu, L. Yang, G. Peng, L. Yang, ARID1A deficiency and immune checkpoint blockade therapy: From mechanisms to clinical application, Cancer Lett. 473 (2020) 148–155, https://doi.org/10.1016/j.canlet.2020.01.001.
[64] R. Okamura, S. Kato, S. Lee, R.E. Jimenez, J.K. Sicklick, R. Kurzrock, ARID1A alterations function as a biomarker for longer progression-free survival after anti-PD-1/PD-L1 immunotherapy, J. Immunother. Cancer 8 (1) (2020) e000438.
[65] K. Chen, J. Liu, S. Liu, M. Xia, X. Zhang, D. Han, Y. Jiang, C. Wang, X. Cao, Methyltransferase SETD2-Mediated Methylation of STAT1 Is Critical for Interferon Antiviral Activity, Cell 170 (3) (2017) 492–506.e14.
[66] Y. Hu, X. Wang, J. Song, J. Wu, J. Xu, Y. Chai, Y. Ding, B. Wang, C. Wang, Y. Zhao, Z. Shen, X. Xu, X. Cao, Chromatin remodeler ARID1A binds IRF3 to selectively induce antiviral interferon production in macrophages, Cell Death Dis. 12 (8) (2021) 743, https://doi.org/10.1038/s41419-021-04032-9.
[67] A.M. Sarshekeh, J. Roszik, G.C. Manyam, S.M. Advani, J. Willis, J.P.Y.C. Shen, J. Morris, J.S. Davis, J.A. Ajani, D.M. Maru, M.J. Overman, S. Kopetz, ARID1A mutation to define an immunologically active subgroup in patients with microsatellite-stable colorectal cancer, J. Clin. Oncol. 38 (4_suppl) (2020) 215, https://doi.org/10.1200/JCO.2020.38.4_suppl.215.
[68] Q. Jiang, X. Huang, X. Hu, Z. Shan, Y. Wu, G. Wu, L. Lei, Histone demethylase KDM6A promotes somatic cell reprogramming by epigenetically regulating the PTEN and IL-6 signal pathways, Stem. Cells 38 (8) (2020) 960–972, https://doi.org/10.1002/stem.3188.
[69] S. Lerrer, Y. Liubomirski, A. Bott, K. Abnaof, N. Oren, A. Yousaf, C. Korner, T. Meshel, S. Wiemann, A. Ben-Baruch, Co-Inflammatory Roles of TGFbeta1 in the Presence of TNFalpha Drive a Pro-inflammatory Fate in Mesenchymal Stem Cells, Front. Immunol. 8 (2017) 479, https://doi.org/10.3389/fimmu.2017.00479.
[70] T. Korn, M. Mitsdoerffer, A.L. Croxford, A. Awasthi, V.A. Dardalhon, G. Galileos, P. Vollmar, G.L. Stritesky, M.H. Kaplan, A. Waisman, V.K. Kuchroo, M. Oukka, IL-6 controls Th17 immunity in vivo by inhibiting the conversion of conventional T cells into Foxp3+ regulatory T cells, PNAS 105 (47) (2008) 18460–18465, https://doi.org/10.1073/pnas.0809850105.
[71] S. Dominitzki, M.C. Fantini, C. Neufert, A. Nikolaev, P.R. Galle, Jürgen Scheller, G. Monteleone, S. Rose-John, M.F. Neurath, C. Becker, Cutting edge: trans-signaling via the soluble IL-6R abrogates the induction of FoxP3 in naive CD4+ CD25 T cells, J. Immunol. 179 (4) (2007) 2041–2045.
[72] E. Bettelli, Y. Carrier, W. Gao, T. Korn, T.B. Strom, M. Oukka, H.L. Weiner, V. K. Kuchroo, Reciprocal developmental pathways for the generation of pathogenic effector TH17 and regulatory T cells, Nature 441 (7090) (2006) 235–238, https://doi.org/10.1038/nature04753.
[73] J. Ye, R.S. Livergood, G. Peng, The role and regulation of human Th17 cells in tumor immunity, Am. J. Pathol. 182 (1) (2013) 10–20, https://doi.org/10.1016/j.ajpath.2012.08.041.
[74] A. Alsuliman, D. Colak, O. Al-Harazi, H. Fitwi, A. Tulbah, T. Al-Tweigeri, M. Al-Alwan, H. Ghebeh, Bidirectional crosstalk between PD-L1 expression and epithelial to mesenchymal transition: significance in claudin-low breast cancer cells, Mol. Cancer 14 (2015) 149, https://doi.org/10.1186/s12943-015-0421-2.
[75] Y. Lou, L. Diao, E.R. Cuentas, W.L. Denning, L. Chen, Y.H. Fan, L.A. Byers, J. Wang, V.A. Papadimitrakopoulou, C. Behrens, J.C. Rodriguez, P. Hwu, Wistuba, II, J.V. Heymach, D.L. Gibbons, Epithelial-Mesenchymal Transition Is Associated with a Distinct Tumor Microenvironment Including Elevation of Inflammatory Signals and Multiple Immune Checkpoints in Lung Adenocarcinoma, Clin Cancer Res 22 (14) (2016) 3630-42. doi:10.1158/1078-0432.CCR-15-1434.
[76] Y. Manjunath, S.V. Upparahalli, D.M. Avella, C.B. Deroche, E.T. Kimchi, K.F. Staveley-O'Carroll, C.J. Smith, G. Li, J.T. Kaifi, PD-L1 Expression with Epithelial Mesenchymal Transition of Circulating Tumor Cells Is Associated with Poor Survival in Curatively Resected Non-Small Cell Lung Cancer, Cancers (Basel) 11(6) (2019). doi:10.3390/cancers11060806.
[77] K. Dhatchinamoorthy, J.D. Colbert, K.L. Rock, Cancer Immune Evasion Through Loss of MHC Class I Antigen Presentation, Front. Immunol. 12 (2021), 636568, https://doi.org/10.3389/fimmu.2021.636568.
[78] A. Dongre, M. Rashidian, F. Reinhardt, A. Bagnato, Z. Keckesova, H.L. Ploegh, R. A. Weinberg, Epithelial-to-Mesenchymal Transition Contributes to Immunosuppression in Breast Carcinomas, Cancer Res. 77 (15) (2017) 3982–3989.
[79] J. Chu, F. Gao, M. Yan, S. Zhao, Z. Yan, B. Shi, Y. Liu, Natural killer cells: a promising immunotherapy for cancer, J. Transl. Med. 20 (1) (2022) 240, https://doi.org/10.1186/s12967-022-03437-0.
[80] C. Marbaniang, L. Kma, Dysregulation of Glucose Metabolism by Oncogenes and Tumor Suppressors in Cancer Cells, Asian Pac. J. Cancer Prev. 19 (9) (2018) 2377–2390, https://doi.org/10.22034/APJCP.2018.19.9.2377.
[81] E. Madden, S.E. Logue, S.J. Healy, S. Manie, A. Samali, The role of the unfolded protein response in cancer progression: From oncogenesis to chemoresistance, Biol. Cell 111 (1) (2019) 1–17, https://doi.org/10.1111/boc.201800050.